



Editor-in-Chief:

Miaoqing Zhao, PhD., MD (Shandong First Medical University, Jinan, China)

Co-editor-in-Chief:

Lester J. Layfield, MD, (University of Missouri, Columbia, MO, USA)

Founding Editor & Editor-in-chief Emeritus:

Vinod B. Shidham, MD, FIAC, FRCPath (WSU School of Medicine, Detroit, USA)

Research Article

# Inhibition of CXCR2 as a therapeutic target for chronic post-surgical pain: Insights from animal and cell models

Jiacheng Zhao, MM<sup>1#</sup>, Chenlu Jian, MM<sup>1#</sup>, Zhusheng Chen, MM<sup>1</sup>, Jiawei Cai, MM<sup>1</sup>, Can Zhou, MM<sup>1</sup>, Ming Li, MM<sup>1</sup>, Yang Yang, MD<sup>2</sup>, Yongtao Gao, MM<sup>1</sup>

<sup>1</sup>Department of Anesthesiology, Affiliated Hospital of Nantong University, Medical School of Nantong University, Nantong, The People's Republic of China.

<sup>2</sup>Department of Emergency Medicine, Affiliated Hospital of Nantong University, Nantong, The People's Republic of China.

\*These authors contributed equally to this work



\*Corresponding author:

Yongtao Gao  
Department of Anesthesiology,  
Affiliated Hospital of Nantong  
University, Medical School of  
Nantong University, Nantong,  
The People's Republic of China.

[gyt19700114@sina.com](mailto:gyt19700114@sina.com)

Yang Yang,  
Department of Emergency  
Medicine, Affiliated Hospital of  
Nantong University, Nantong,  
The People's Republic of China.

[yangyang286228@ntu.edu.c](mailto:yangyang286228@ntu.edu.c)

Received: 18 April 2024

Accepted: 29 April 2024

Published: 29 August 2024

DOI

[10.25259/Cytojournal\\_46\\_2024](https://doi.org/10.25259/Cytojournal_46_2024)

Quick Response Code:



Supplementary material  
associated with this article can  
be found on:

[https://dx.doi.org/10.25259/  
Cytojournal\\_46\\_2024](https://dx.doi.org/10.25259/Cytojournal_46_2024)



Publisher of Scientific Journals

## ABSTRACT

**Objective:** Studies have shown that chemokines can stimulate the migration and activation of microglia to cause chronic post-surgical pain (CPSP). However, the involvement of C-X-C motif chemokine receptor 2 (CXCR2) as a new chemotactic factor in regulating CPSP and its underlying mechanism remains unclear. This study is to investigate the role of CXCR2 in the development of CPSP and reveal the underlying mechanism.

**Material and Methods:** A rat model of skin/muscle incision and retraction was established, and treated with or without SB225002 (a selective inhibitor of CXCR2). In addition, the primary microglia cells induced by lipopolysaccharide were applied as an *in vitro* model for CPSP and treated individually with si-negative control (NC), si-CXCR2, si-CXCR2+Interleukin (IL)-6 (an agonist of the janus kinase (JAK)/signal transducers and activators of transcription (STAT)3 signaling pathway), si-CXCR2+IL-6+si-NC, or si-CXCR2+IL-6+si-exchange protein 1 directly activated by cAMP (EPAC1).

**Results:** Results from the database analysis showed that CXCR2 and JAK/STAT3 signaling pathway-related genes, including JAK1, STAT3, and EPAC1, were mainly involved in the development of CPSP. Inhibition of CXCR2 expression not only inhibited the reduction of foot pain threshold in CPSP models but also led to a decreased expression of CXCR2 and the phosphorylation levels of JAK and STAT3 in both animal and cell models. Furthermore, inhibition of EPAC1 expression can hinder the regulatory function of CXCR2.

**Conclusion:** This study indicated that the high expression of CXCR2 activates the JAK1/STAT3 signaling pathway, enhances EPAC1 activation in microglial cells, and exacerbates CPSP.

**Keywords:** C-X-C motif chemokine receptor 2, Exchange protein 1 directly activated by cAMP, Chronic post-operative pain, Signaling pathway

## INTRODUCTION

Pain is a perceptual discomfort and emotional experience associated with actual or latent organ damage,<sup>[1]</sup> which originates from a variety of complex neural mechanisms exogenous to the entire spinal cord and brain tissue,<sup>[2]</sup> among which CPSP, defined as pain in and around the surgical area for more than 2 months, excluding causes such as disease recurrence or inflammation,<sup>[3]</sup> as a prevalent complication, posing a persistent challenge for effective treatment.<sup>[4]</sup> A previous study showed that 75% of patients who had undergone major surgery developed CPSP,<sup>[5]</sup> while 70% reported persistent pain despite taking painkillers. Therefore, improving post-operative analgesia is essential to reduce post-operative morbidity and mortality rates. Methods for controlling

This is an open-access article distributed under the terms of the Creative Commons Attribution-Non Commercial-Share Alike 4.0 License, which allows others to remix, transform, and build upon the work non-commercially, as long as the author is credited and the new creations are licensed under the identical terms. © 2024 The Author(s). Published by Scientific Scholar.

CPSP include drug therapy, anesthesia, cognitive therapy, and behavioral methods.<sup>[6,7]</sup> However, effective prevention and treatment measures for CPSP remain elusive, and its pathogenesis is complex.

CPSP is neuropathic pain caused by peripheral neurosurgical trauma.<sup>[8]</sup> Studies have shown that a chemotactic factor related to peripheral nervous system diseases, microsecretory chemotactic protein, can promote the progression of neuroinflammation and cause CPSP.<sup>[9]</sup> Furthermore, chemotactic factors stimulate the migration and activation of microglial cells, thereby regulating neuropathic pain.<sup>[10]</sup> Among them, CXCR2, as a novel chemokine, not only promotes the local immune response, especially the recruitment and activation of neutrophils,<sup>[11]</sup> but also plays a crucial role in mediating inflammation and neuropathic pain.<sup>[12]</sup> Other studies have shown that CXCR2 is highly expressed in a chronic compressive injury-induced neuropathic pain model,<sup>[13,14]</sup> and SB225002, a specific CXCR2 antagonist, significantly inhibited the microglial activity and production of proinflammatory cytokines in cultured microglia exposed to lipopolysaccharide (LPS), effectively alleviated mechanical and cold hypersensitivity in the aftermath of peripheral nerve injury.<sup>[14]</sup>

The inhibition of JAK1/STAT3 signaling pathway has shown potential in alleviating neuropathic pain caused by both inflammatory and non-inflammatory mechanisms<sup>[15,16]</sup> and has been identified as a drug target for chronic pain through transcriptomics.<sup>[17]</sup> Moreover, the increased guanine nucleotide exchange protein conversion factor (GEFs) directly regulated by cAMP (cAMP-GEF, EPAC, Epac)1 signaling is a factor in CPSP. This study indicated that the high expression of CXCR2 activates the JAK1/STAT3 signaling pathway, enhances EPAC1 activation in microglial cells, and exacerbates CPSP.<sup>[18-22]</sup>

Thus, we hypothesized that CXCR2 activates the JAK1/STAT3 signaling pathway, improves EPAC1 expression, and activates microglia to aggravate CPSP. This study utilized *in vivo* and *in vitro* models of CPSP to investigate the effects of CXCR2 on the development of CPSP and its underlying mechanisms.

## MATERIAL AND METHODS

### Animal experiments

Adult Sprague-Dawley (SD) rats (male, 200–240 g, 40 in total) were housed in plastic cages (5 rats in a cage) with sawdust as bedding and supplied with food and drinking water. The animals were kept under controlled conditions of 50% humidity, a temperature of 25°C, and a 12-h light-dark cycle. We established a CPSP rat model similar to clinical operations through femoral incision traction. Under general anesthesia, two small traction devices were cut from the inside of the thigh to the surface muscles. Stretch the tissue for an hour,

which may stretch the sciatic nerve. The pain performance of skin/muscle incision and retraction (SMIR) rats were evaluated by measuring the stimulation of the hindfoot and the contraction process. The first experiment was divided into two groups randomly: Control and Model, and the second experiment was divided into three groups randomly: Control, Model, and Model+SB225002. Eight animals from each group were tested in parallel, and the test was repeated three times. The CPSP rats were randomly assigned to Model and model+SB225002, and rats without SMIR served as controls. For SB225002 (S7651, Selleck, Houston, TX, USA) treatment, the rats were anesthetized using 2% isoflurane (26675-46-7, Solvay Solutions UK Ltd., UK). The skin around the waist was shaved and sterilized. The L5-L6 vertebral space was located by palpation. A 29-gauge needle (B-D Inc., Toledo, OH, USA) was used to inject 10 µg of SB225002 into this space. A tail-flick reaction confirmed a successful injection.<sup>[23]</sup> After treatment, the rats were anesthetized with 1.5% sevoflurane (Shanghai Hengrui Pharmaceutical Co., Ltd., Shanghai, China) inhalation and euthanized with 50% carbon dioxide volume/min. Serum was taken at the end of the *in vivo* experimental treatment and before carbon dioxide asphyxia after anesthesia for subsequent assays. This ensured that the rats were painless. The dorsal horn of the spinal cord was extracted for further analysis.

The ethical standard of experiments was in accordance with the guidelines provided by the Committee for the Purpose of Control and Supervision of Experiments on Animals (CPCSEA), and all the procedures were approved by the Animal Ethics Committee of the Laboratory Animal Center of Nantong University (IACUC20230215-1004).

### Paw withdrawal threshold (PWT) test

The PWT test using von Frey filaments (37450-275, Ugo Basile, Italy) was conducted at 9:00 am on days 0, 1, 4, 7, 14, and 21. The rats were placed in transparent boxes with grid bottoms and acclimated for 40 min. Different weights of von Frey filaments (2 and 15 g) were applied to the right hind paw for a maximum of 3 s. Positive responses such as sudden withdrawal, shaking, and licking were recorded. The PWT was determined as the minimum force required to elicit a positive response in at least three out of five trials.

### Immunofluorescence

Spinal dorsal horn tissue was fixed with 4% paraformaldehyde (P0099-500 mL, Beyotime, China) for 24 h at room temperature, and sections were permeabilized with 0.2% Triton X-100 (ST797-500 ML, Beyotime, China) solution for 20 min at room temperature. Sections were washed with phosphate-buffered saline (PBS) (C0221A, Beyotime, China) (3 × 10 min, China) and blocked with bovine serum

albumin (BSA) (ST2249-100 g, Beyotime, China) for 2 h at room temperature. Primary antibodies against Iba1 (17198S, CST, USA. Diluted 1:100) were then incubated overnight at 4°C. After washing with PBS, it was ligated to goat secondary antibody (4412S, Alexa Fluor® 488 Conjugate, CST, USA. Diluted 1:500). Nuclei were stained with 4', 6-diamidino-2-phenylindole (DAPI) (C1002, Beyotime, China). Finally, the image was taken under a Zeiss fluorescence microscope (Zeiss, Oberkochen, Germany). The results of all immunofluorescence experiments were quantitatively counted by ImageJ (V.1.8.0, LOCI, University of Wisconsin, Madison, WI, USA) and statistical graphs drawn by GraphPad Prism 9 (Dotmatics, Boston, MA, USA).

### Cell culture and treatment

Primary microglial cells were isolated from the sham-operated rats. Spinal cord tissue was dissected and immersed in Hanks' Balanced Salt Solution (14025076, ThermoFisher, Waltham, MA, USA). After mincing the tissue into 1 mm pieces and filtering it through a 100 µm nylon mesh, the cells were centrifuged at 3000 g for 5 min. The supernatant was discarded and resuspended in complete medium to obtain mixed glial cells. After being cultured in culture dishes for a period of time, microglia cells were purified by the Differential Adherence Method. The purified microglia cells (with no mycoplasma detected) were resuspended in complete Dulbecco's Modified Eagle Medium (DMEM) (C0891-500 mL, Beyotime, China) and plated in 6-well plates at a density of  $3 \times 10^5$  cells/well. The cells were then cultured for two weeks. Once the cells reached 95% confluence, a proinflammatory response was induced by adding LPS (ST1470-50 mg, Beyotime, China) at a 100 ng/mL concentration. Using Lipofectamine 2000 (11668500, ThermoFisher, Waltham, MA, USA), LPS-induced primary microglia cells ( $1 \times 10^5$  cells/well) were transfected with si-CXCR2 or si-EPAC1 (Ruibo Bio Co., Ltd., Guangzhou, China) for 24 h at 37°C. The cells were divided into seven groups: control, LPS, LPS+si-NC, LPS+si-CXCR2, LPS+si-CXCR2+Interleukin (IL)-6 (30 ng/mL), LPS+si-CXCR2+IL-6 (30 ng/mL)+si-NC, and LPS+si-CXCR2+IL-6 (30 ng/mL)+si-EPAC1. Cells were then collected to analyze cell function, and RNA and proteins were extracted from the cells for gene expression analysis. The sequence of siRNA is as follows: si-NC 5'-AAAUUACUUGAGGCACAGUAU-3', si-CXCR2-001 5'-GGAUUAAGUUUACCUCAAAGA-3', si-CXCR2-002 5'-CAGCGAACCUAGAUUCAACA-3', si-CXCR2-003 5'-GUGGAGAUUUGACAGUUACA-3', si-EPAC1-001 5'-GGGUCAGCGUACAGAUGAAGA-3', si-EPAC1-002 5'-CCACAGAGCAUGUGCACAAGG-3', and si-EPAC1-003 5'-CGGAGGGCACGCUGCUCAAUA-3'.

### Primary microglia purity identification

Purified microglia were seeded in 24-well plates at a density of  $10^5$  cells/mL. The microglia were fixed with 4% paraformaldehyde for 15 min at room temperature. After washing, the microglia were permeabilized in 0.3% Triton X-100 for 10 min and blocked with BSA for 1 h. Subsequently, the cells were incubated overnight at 4°C with a primary antibody against CD11b (ab52478, Abcam, Cambridge, UK. Diluted 1:250). Following PBS washing, the microglia were incubated with a Goat Anti-Rabbit IgG H&L (Alexa Fluor® 488) (ab150077, Abcam, Cambridge, UK. Diluted 1:250) for 1 h. Nuclear staining was performed by incubating the cells with DAPI for 90 s. Finally, the preparation was mounted on a slide and imaged using fluorescence microscopy.

### Measurement of IL-1 $\alpha$ and tumor necrosis factor- $\alpha$ (TNF- $\alpha$ ) using enzyme-linked immunosorbent assay (ELISA)

The concentration of IL-1 $\alpha$  (PI563, Beyotime, China) and TNF- $\alpha$  (PT516, Beyotime, China) in spinal dorsal horn tissue or cell supernatant was measured using commercialized ELISA kits based on the operating manual. Absorbance was determined using a microplate reader (BMG LABTECH, Offenburg, Germany).

### 5-ethynyl-2'-deoxyuridine (EdU) assay

Cell proliferation was determined using an EdU assay (C0071L, Beyotime, China). The cells were seeded on a laser scanning plate at a density of  $1 \times 10^6$ . After pretreatment, the cells were incubated with 50 µM EdU buffer 37°C for 120 min. Fixation was carried out using 4% paraformaldehyde, permeabilization with 0.1% Triton X-100, and nuclear staining with DAPI. Tissue sections were prepared using a fluorescence microscope, and the growth rate was analyzed using ImageJ.

### Gene ontology (GO) analysis and Kyoto Encyclopedia of Genes and Genomes database (KEGG) signaling pathway enrichment analysis

GO enrichment analysis and KEGG pathway enrichment analysis were performed using String v12.0 (Available at: <http://stringdb.org>. Accessed: 8 August 2024) to analyze the biological processes and signaling pathways involved in CXCR2 and related genes. Enrichment bubble plot was plotted by <https://www.bioinformatics.com.cn> (Accessed: 7 August 2024), an online platform for data analysis and visualization.

### Integration of the protein-protein interaction (PPI) network

Interactions between CXCR2, JAK1, STAT3, and EPAC1 (RAPGEF3) were analyzed using the STRING database.

Interactions with a combined score of  $>0.700$  were considered statistically significant.

### Quantitative reverse transcription-polymerase chain reaction (PCR)

The RNA was extracted using the TRIzol (15596026, ThermoFisher, Waltham, MA, USA) method and converted to cDNA using a cDNA synthesis kit from Boyotime (D7170L, Boyotime, China). PCR was performed on an ABI 7900 fluorescence quantitative PCR instrument (ABI, USA). Primers were as follows: CXCR2 (rat): 5'-TCTGTTCTTTGCCCTGACCT-3' and 5'-GTACTTGTGGCGTGGACGAT-3', EPAC1 (Rapgef3) (rat): 5'-TCCTCCTGTCATCCCTTTCA-3' and 5'-GCCATCATTCGCATCTTCTCA-3' (shown in Rapgef3 Rap guanine nucleotide exchange factor 3 [Rattus norvegicus (Norway rat)] - Gene - NCBI (nih.gov)),  $\beta$ -actin (rat): 5'-GGGAAATCGTGCATGACATT-3' and 5'-GCGGCAGTGGCCATCTC-3'. The expression of  $\beta$ -actin was used to standardize mRNA expression, employing the  $2^{-\Delta\Delta CT}$  method for calculation.

### Western blotting technique

Proteins were extracted from tissues and cells using radioimmunoprecipitation assay (RIPA) lysis buffer (sc-24948, Santa Cruz Biotechnology, Dallas, TX, USA). The obtained proteins were transferred to a polyvinylidene fluoride film and sealed with 5% skim milk. Subsequently, an antimicrobial agent was added to the polyvinylidene difluoride (PVDF) (FFP28, Beyotime, China.) film at 4°C to make it overnight. The PVDF membranes were then incubated with human or rat polyclonal antibodies for p-JAK1 (74129S, CST, USA. Diluted 1:1000), JAK1 (3344S, CST, USA. Diluted 1:3000), p-STAT3 (9145S, CST, USA. Diluted 1:2000), STAT3 (30835S, CST, USA. Diluted 1:2000), EPAC1 (4155S, CST, USA. Diluted 1:1000), and CXCR2 (ab65968, Abcam, UK. Diluted 1:2000) and  $\beta$ -actin (ab8227, Abcam, UK. Diluted 1:2000), followed by secondary antibody (ab6721, ab97245, Abcam, UK. Diluted 1:5000). Blots were visualized using enhanced chemiluminescence, with  $\beta$ -actin serving as an internal reference protein. Protein expression levels were quantified using the ImageJ software.

### Statistical analysis

Data were analyzed using the SPSS (version 23.0, IBM Corp., Armonk, NY, USA.). Continuous variables were calculated as means and standard deviations. Statistical tests, such as t-tests, one-way analysis of variance, and Least Significant Difference (LSD) tests, were used to compare differences between groups. A significance level of  $P < 0.05$  was considered statistically significant.

## RESULTS

### Establishment and identification of the CPSP model

First, we determined the PWT in the CPSP model group and control group rats. The PWT was significantly reduced in the CPSP model group [ $P < 0.05$ , Figure 1a]. Immunofluorescence analysis revealed an increased microglial cell marker Iba1 level in the CPSP model group [Figure 1b]. The content of IL-1 $\alpha$  and TNF- $\alpha$  in spinal dorsal horn tissue was measured using ELISA. The levels of IL-1 $\alpha$  and TNF- $\alpha$  were significantly increased in the CPSP model group compared to the control group [ $P < 0.001$ , Figure 1c and d].

### Expression and biological function of CXCR2 in the CPSP model

The CXCR2 levels in the CPSP model were analyzed using real-time PCR and demonstrated that CXCR2 levels were increased in the CPSP model [ $P < 0.001$ , Figure 2a]. The protein levels of p-JAK1, JAK1, p-STAT3, STAT3, and EPAC1 were analyzed using western blot analysis. P-JAK1, p-STAT3, and EPAC1 were increased in the CPSP model [ $P < 0.001$ , Figure 2b]. The STRING database (<https://cn.string-db.org/>) was used to analyze the PPI network of CXCR2. STAT3, JAK1, and RAPGEF3 were associated with CXCR2 expression [Figure 2c]. The biological function of CXCR2 was analyzed using GO analysis. We found that the GO functions of CXCR2 were mainly enriched in an inflammatory response and cytokine-mediated signaling pathways [Figure 2d]. KEGG pathway enrichment analysis was performed to explore CXCR2-related pathways. The JAK-STAT signaling pathway was the key enriched pathway related to CXCR2 [Figure 2e].

### Effects of CXCR2 inhibition on PWT; Iba1, IL-1 $\alpha$ , and TNF- $\alpha$ levels; and the JAK1/STAT3 signaling pathway in CPSP model

CPSP rats were treated with SB225002. PWTs in the treated and control groups were measured. The PWT was significantly decreased in CPSP rats ( $P < 0.05$ ); however, this was reversed by SB225002 [ $P < 0.05$ , Figure 3a]. The expression of Iba1 was analyzed using immunofluorescence and was found to be increased in CPSP rats but decreased after treatment with SB225002 [Figure 3b]. IL-1 $\alpha$  and TNF- $\alpha$  levels were measured using ELISA in spinal dorsal horn tissue. CPSP rats showed higher levels of IL-1 $\alpha$  and TNF- $\alpha$  than these elevated levels [ $P < 0.001$ , Figure 3c and d]. The p-JAK1, JAK1, p-STAT3, STAT3, and EPAC1 levels were analyzed using western blot analysis. CPSP rats exhibited increased levels of p-JAK1, p-STAT3, and EPAC1 ( $P < 0.001$ ), which were reversed by SB225002 treatment [ $P < 0.001$ ; Figure 3e].

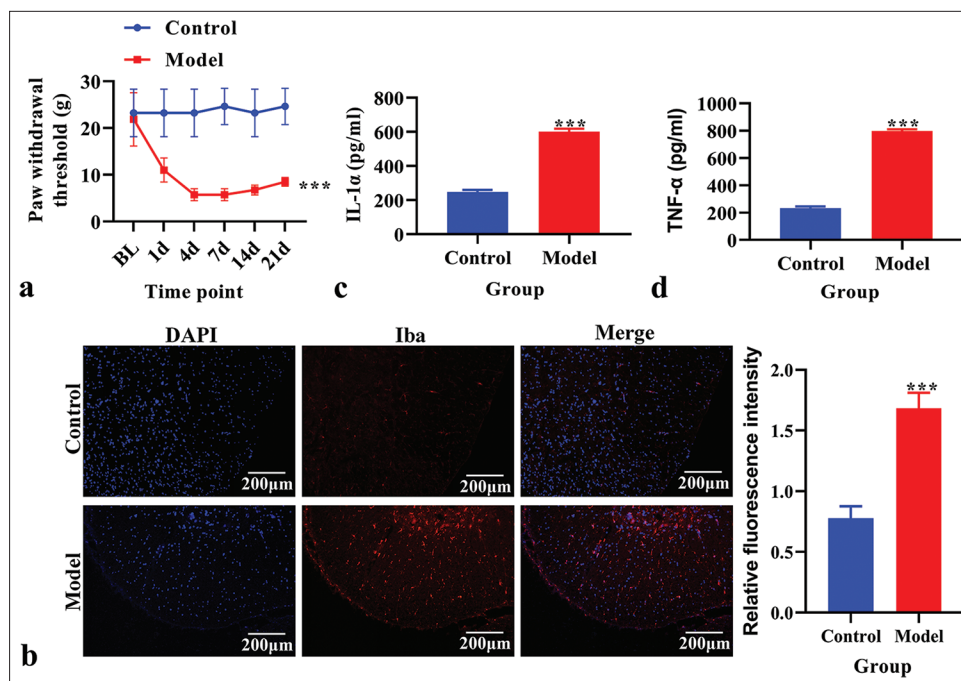


**Figure 1:** The establishment and identification of an *in vivo* model of chronic post-surgical pain. (a) Paw withdrawal threshold. (b) The expression of Ionized calcium binding adaptor molecule 1 (Iba1) analyzed using immunofluorescence. Red fluorescence indicates Iba1. Blue fluorescence indicates the nucleus. (c) The level of Interleukin-1 $\alpha$  analyzed using enzyme-linked immunosorbent assay (ELISA). (d) The level of tumor necrosis factor- $\alpha$  analyzed using ELISA. \*\*\* $P < 0.001$  versus Control. TNF: Tumor necrosis factor

#### Effects of CXCR2 knockdown on cell proliferation, IL-1 $\alpha$ and TNF- $\alpha$ levels, and the JAK1/STAT3 signaling pathway in LPS-induced primary microglia cells

Before *in vitro* experiments, the purity of primary microglia was identified by immunofluorescence using the specific marker CD11b, and the purity of primary cultured microglia was found to be higher than 90% [Figure 4a]. CXCR2 levels were analyzed using real-time PCR to verify the CXCR2 knockdown efficiency. The knockdown efficiency of si-CXCR2-002 was the highest [ $P < 0.001$ , Figure S1a]. The mRNA level of CXCR2 was increased in LPS-induced primary microglial cells ( $P < 0.001$ ), but decreased after transfection with si-CXCR2 [ $P < 0.001$ , Figure 4b]. The protein level of CXCR2, as analyzed using western blot analysis, was also increased ( $P < 0.001$ ), which was reversed by si-CXCR2 [ $P < 0.001$ , Figure 4c]. Cell proliferation, assessed using the EdU assay, increased in the LPS and LPS+si-NC groups but was reversed by si-CXCR2 [Figure 4d]. The level of IL-1 $\alpha$  and TNF- $\alpha$  in the cell supernatant, measured using ELISA, was higher in the LPS group compared to the control group ( $P < 0.001$ ) but reversed by si-CXCR2 [ $P < 0.001$ , Figure 4e and f]. The levels of p-JAK1, JAK1, p-STAT3, STAT3, and EPAC1, as analyzed using western blot analysis, were increased in LPS-induced primary microglial cells ( $P < 0.05$ ) but were reversed by si-CXCR2 [ $P < 0.001$ , Figure 4g].

#### Effects of IL-6 on cell proliferation, IL-1 $\alpha$ and TNF- $\alpha$ levels, and the JAK1/STAT3 signaling pathway in LPS-induced primary microglia cells transfected with si-CXCR2

The p-JAK1, JAK1, p-STAT3, STAT3, and EPAC1 levels were analyzed using western blot analysis. The levels of p-JAK1, p-STAT3, and EPAC1 were lower in the LPS+si-CXCR2 group compared to the LPS+si-NC group ( $P < 0.001$ ), and these levels were reversed by IL-6 treatment [ $P < 0.001$ , Figure 5a]. Cell proliferation, as assessed using EdU assay, was decreased in the LPS+si-NC group ( $P < 0.001$ ), and these levels were reversed by IL-6 treatment [ $P < 0.001$ , Figure 5b]. The concentrations of IL-1 $\alpha$  and TNF- $\alpha$  in cell supernatant were detected by ELISA assay. The results showed that IL-1 $\alpha$  and TNF- $\alpha$  were significantly reduced in the LPS+si-CXCR2 group compared to the LPS+si-NC group, and these effects were reversed by IL-6 [ $P < 0.001$ , Figure 5c and d].

#### Effects of EPAC1 knockdown on cell proliferation and levels of IL-1 $\alpha$ and TNF- $\alpha$ in LPS-induced primary microglia cells treated with si-CXCR2 and IL-6

EPAC1 expression was analyzed using real-time PCR to confirm the EPAC1 knockdown efficiency. The knockdown efficiency of si-EPAC1-001 was the highest [ $P < 0.001$ , Figure S1b]. The results showed that the expression of EPAC1

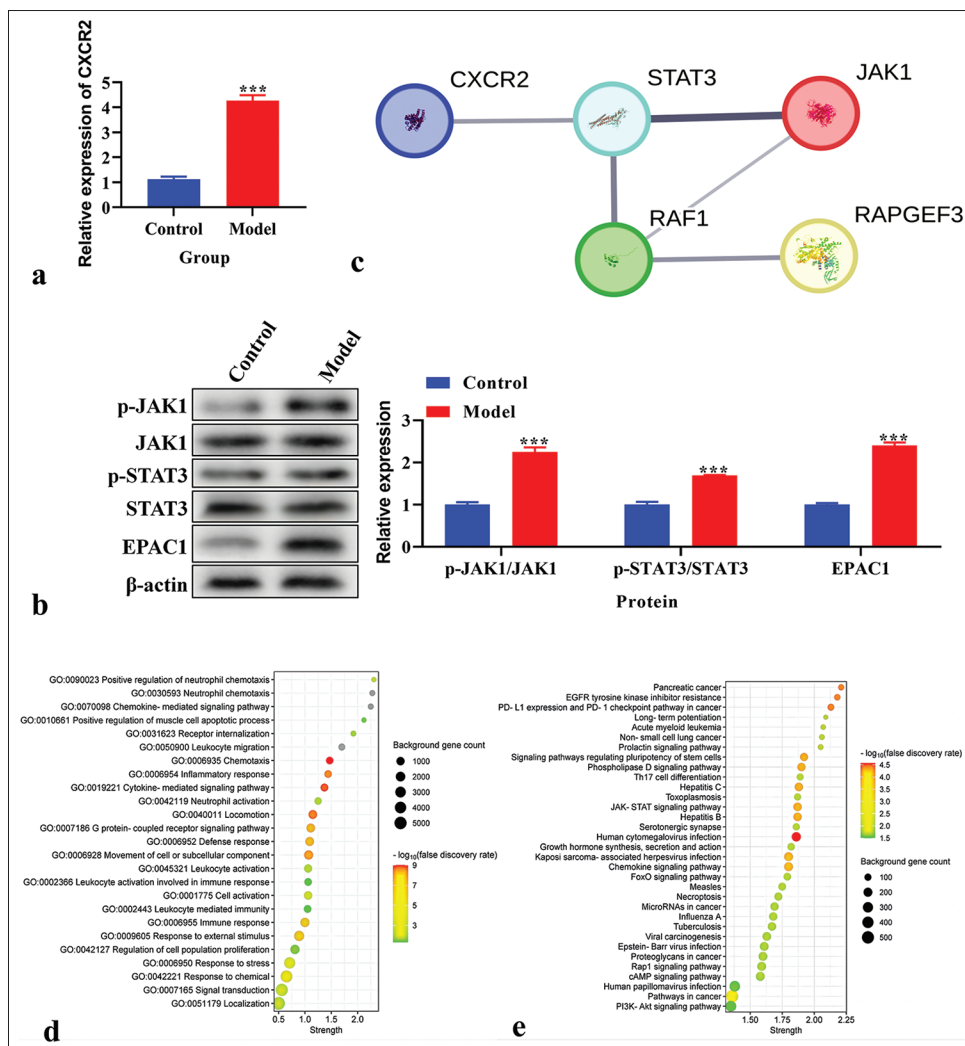


**Figure 2:** Expression and biological function of C-X-C motif chemokine receptor 2 (CXCR2) in chronic post-surgical pain model. (a) The expression of CXCR2 using real-time polymerase chain reaction. (b) The expression of p-Janus Kinase (JAK), JAK1, p-signal transducers and activators of transcription (STAT), STAT3, and exchange protein 1 directly activated by cAMP (EPAC1) using western blot. (c) Protein-protein interaction network of CXCR2. Line thickness indicates the strength of data support. (d) Gene ontology analysis of CXCR2. (e) Kyoto encyclopedia of genes and genomes pathway enrichment analysis of CXCR2. \*\*\* $P < 0.001$  versus Control.

was significantly reduced in the si-EPAC1 group compared with the si-NC group [ $P < 0.001$ , Figure 6a]. Western blot analysis confirmed a decrease in EPAC1 levels following treatment with si-EPAC1 compared to those in the LPS+si-CXCR2+IL-6 group [Figure 6b]. As assessed using EdU assay, cell proliferation showed that si-EPAC1 reversed the increased cell proliferation observed in the LPS+si-CXCR2+IL-6 group [Figure 6c]. The concentration of IL-1 $\alpha$  and TNF- $\alpha$  in the cell supernatant, measured using ELISA, was lower in the LPS+si-CXCR2+IL-6+si-EPAC1 group compared to the LPS+si-CXCR2+IL-6 group [ $P < 0.001$ , Figure 6d and e].

## DISCUSSION

CPSP refers to persistent pain lasting for more than 2 months that occurs after a surgical procedure<sup>[24]</sup> which is a global concern that affects patients worldwide.

In this study, we used a rat CPSP model to conduct *in vivo* experiments, as it was reported that an SMIR model was usually the CPSP model.<sup>[25]</sup> SMIR surgery resulted in a significant reduction in the ipsilateral PWT by 50% in the CPSP model,<sup>[26]</sup> and we found that the PWT was decreased in CPSP rats, consistent with the previous literature findings.<sup>[26]</sup> In addition, our study revealed increased levels of Iba1 and content of IL-1 $\alpha$  and TNF- $\alpha$  in the CPSP model, consistent

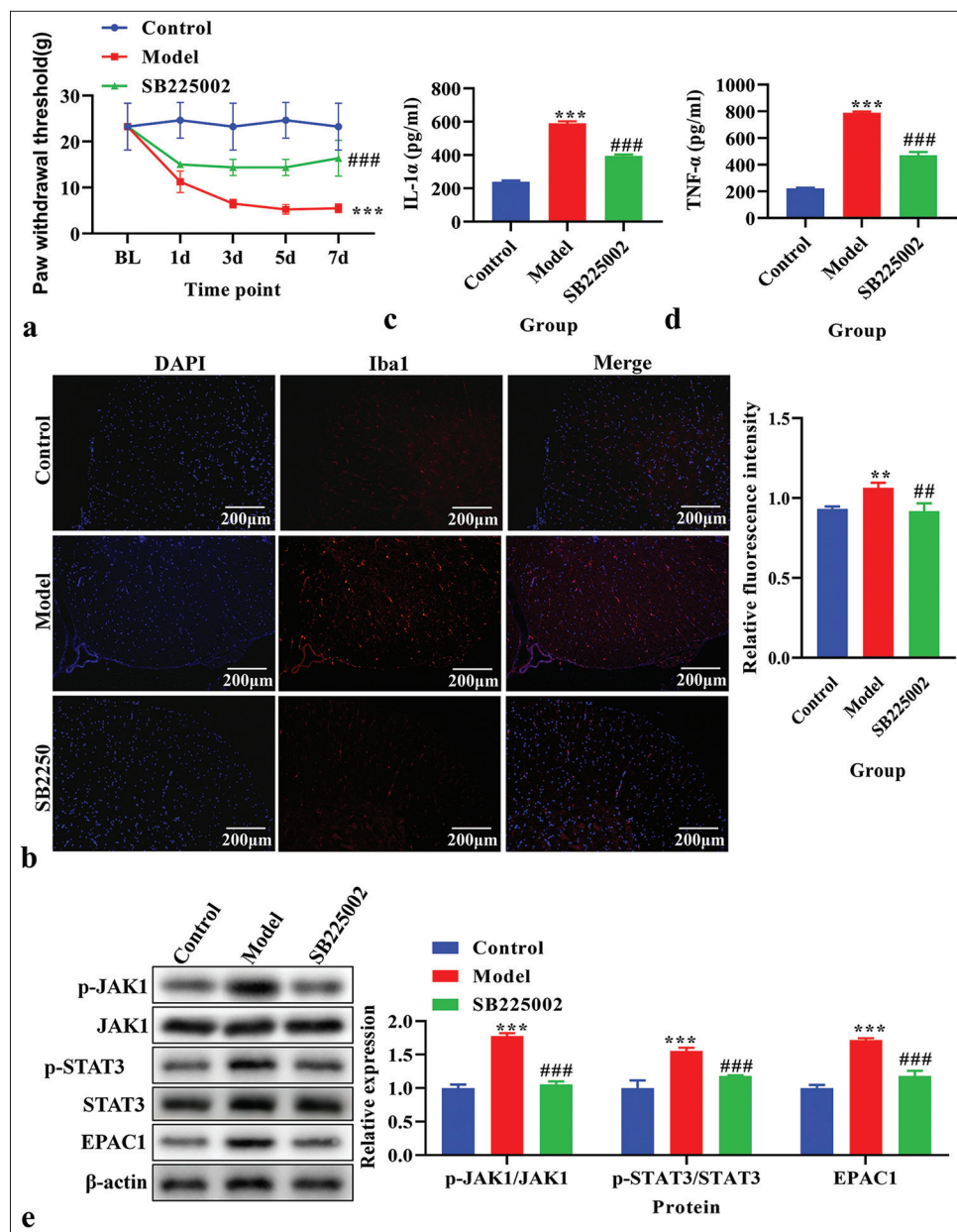


**Figure 3:** The effects of inhibition of C-X-C motif chemokine receptor 2 on paw withdrawal threshold (PWT), the level of Ionized calcium binding adaptor molecule 1 (Iba1), interleukin (IL)-1 $\alpha$ , and tumor necrosis factor- $\alpha$  (TNF- $\alpha$ ), and Janus Kinase (JAK)/signal transducers and activators of transcription (STAT) signaling pathway *in vivo*. (a) PWT. (b) The expression of Iba1 using immunofluorescence. Red fluorescence indicates Iba1. Blue fluorescence indicates the nucleus. (c) The level of IL-1 $\alpha$  using enzyme-linked immunosorbent assay (ELISA). (d) The level of TNF- $\alpha$  using ELISA. (e) The expression of p-JAK1, JAK1, p-STAT3, STAT3, and exchange protein 1 directly activated by cAMP (EPAC1) using western blot. \*\* $P < 0.01$  \*\*\* $P < 0.001$  versus Control, ### $P < 0.001$  versus Model.

with previous studies' findings.<sup>[8,27]</sup> These results confirmed the successful establishment of the CPSP rat model, while a more comprehensive model representation is needed to make the conclusions of this paper more convincing.

CXCR2 expression is increased in CPSP rats, and CXCR2 inhibitor SB225002 can reverse the decrease of PWT and

the increase of IL-1 $\alpha$  and TNF- $\alpha$  levels in CPSP model rats, suggesting that CXCR2 is involved in the occurrence and development of CPSP. In addition, we performed GO and KEGG pathway enrichment analyses, which are typically used to analyze the key metabolic pathways or functions of differentially expressed genes,<sup>[28]</sup> to explore the key

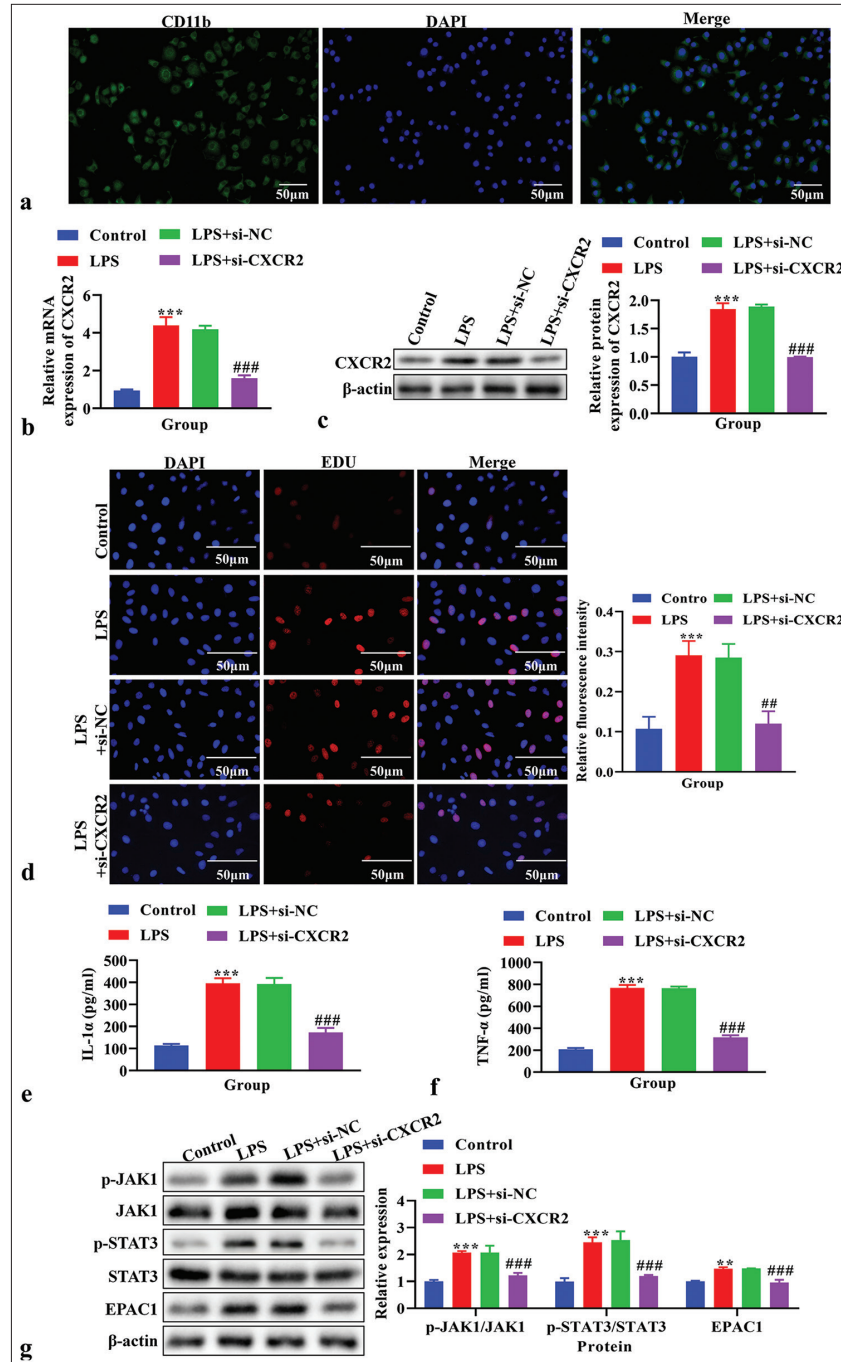


**Figure 4:** The effects of knockdown C-X-C motif chemokine receptor 2 (CXCR2) on cell proliferation, the level of interleukin (IL)-1 $\alpha$  and tumor necrosis factor- $\alpha$  (TNF- $\alpha$ ), and Janus Kinase (JAK)/signal transducers and activators of transcription (STAT) signaling pathway *in vitro*. (a) The purity of primary microglia was identified by immunofluorescence. Blue signal indicates nuclei stained with 4', 6-diamidino-2-phenylindole; the green signal indicates CD11b stained with FITC. (b) The expression of CXCR2 using real-time polymerase chain reaction. (c) The expression of CXCR2 using western blot. (d) Cell proliferation using 5-ethynyl-2'-deoxyuridine (EdU) assay. (e) The level of IL-1 $\alpha$  using enzyme linked immunosorbent assay (ELISA). (f) The level of TNF- $\alpha$  using ELISA. (g) The expression of p-JAK1, JAK1, p-STAT3, STAT3 and exchange protein 1 directly activated by cAMP (EPAC1) using western blot. \*\* $P < 0.01$ , \*\*\* $P < 0.001$  versus Control, ## $P < 0.01$ ### $P < 0.001$  versus LPS+si-NC.



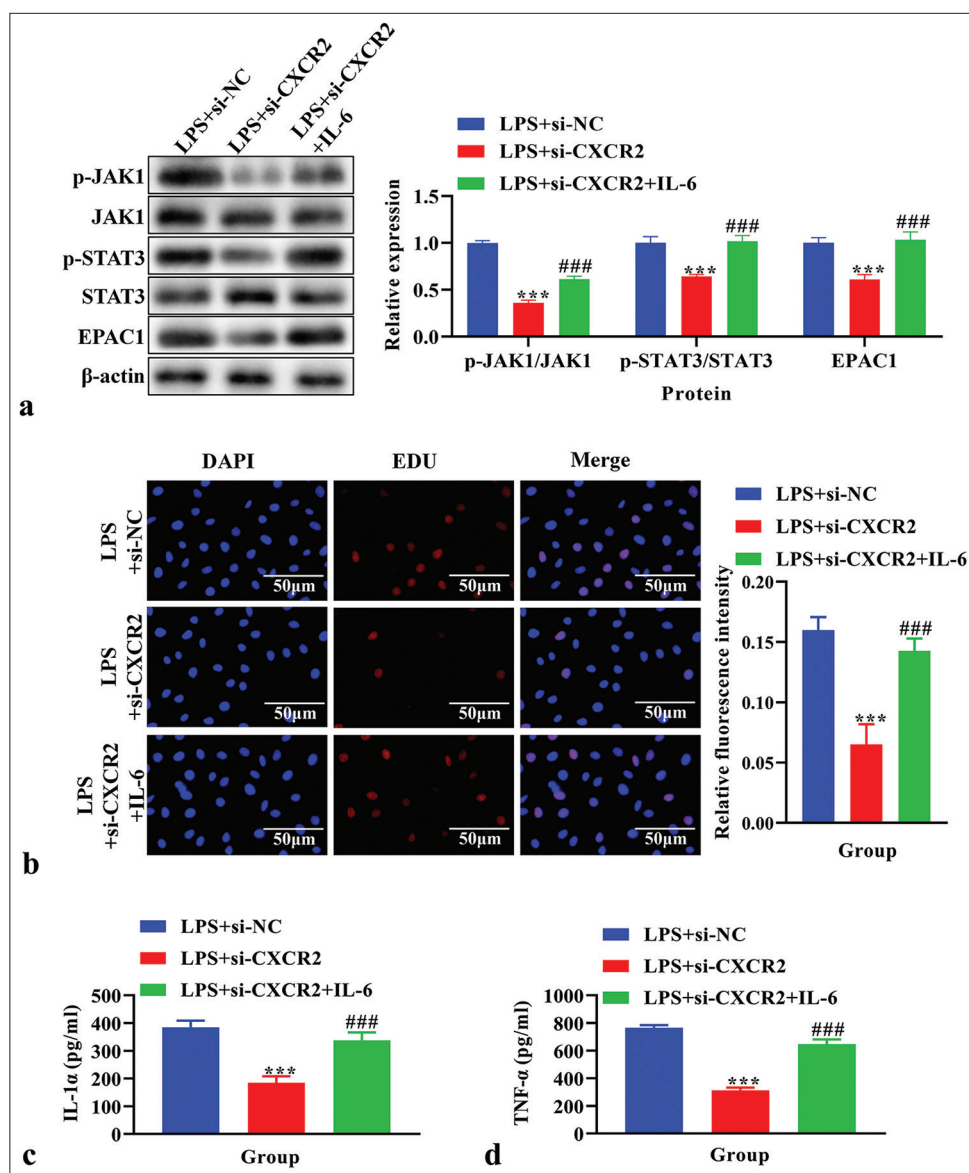


**Figure 5:** The effects of interleukin (IL)-6 on cell proliferation, the level of IL-1 $\alpha$  and tumor necrosis factor- $\alpha$  (TNF- $\alpha$ ), and Janus Kinase (JAK)/signal transducers and activators of transcription (STAT) signaling pathway in lipopolysaccharide (LPS)-induced primary microglia cells transfected with si-C-X-C motif chemokine receptor 2 (CXCR2). (a) The expression of p-JAK1, JAK1, p-STAT3, STAT3, and exchange protein 1 directly activated by cAMP (EPAC1) using western blot. (b) Cell proliferation using EdU assay. (c) The level of IL-1 $\alpha$  using enzyme-linked immunosorbent assay (ELISA). (d) The level of TNF- $\alpha$  using ELISA. \*\*\* $P < 0.001$  versus LPS+si-NC, ### $P < 0.001$  versus LPS+si-CXCR2.

functions and pathways associated with CXCR2 and the STRING database to identify the PPI network of CXCR2, finding that the inflammatory response and the JAK-STAT signaling pathway were key functions and pathways related to CXCR2 and the key genes (STAT3, JAK1, and rap guanine exchange factor (RAPGEF)3 [EPAC1]) were closely related to CXCR2 expression. We also found that p-JAK1, p-STAT3, and EPAC1 levels were increased in the CPSP model but were reversed by SB225002, confirming

that CXCR2 may activate the JAK-STAT signaling pathway in the CPSP model.

To determine the role of CXCR2 in CPSP pathogenesis, an *in vitro* study was conducted using LPS-induced primary microglial cells, which are common *in vitro* models for studying CPSP<sup>[29]</sup> and found the level of CXCR2, IL-1 $\alpha$ , TNF- $\alpha$ , and the expression of JAK-STAT signaling pathway-related genes (STAT3, JAK1, and EPAC1) were all increased, while reversed by CXCR2 knockdown, which was consistent

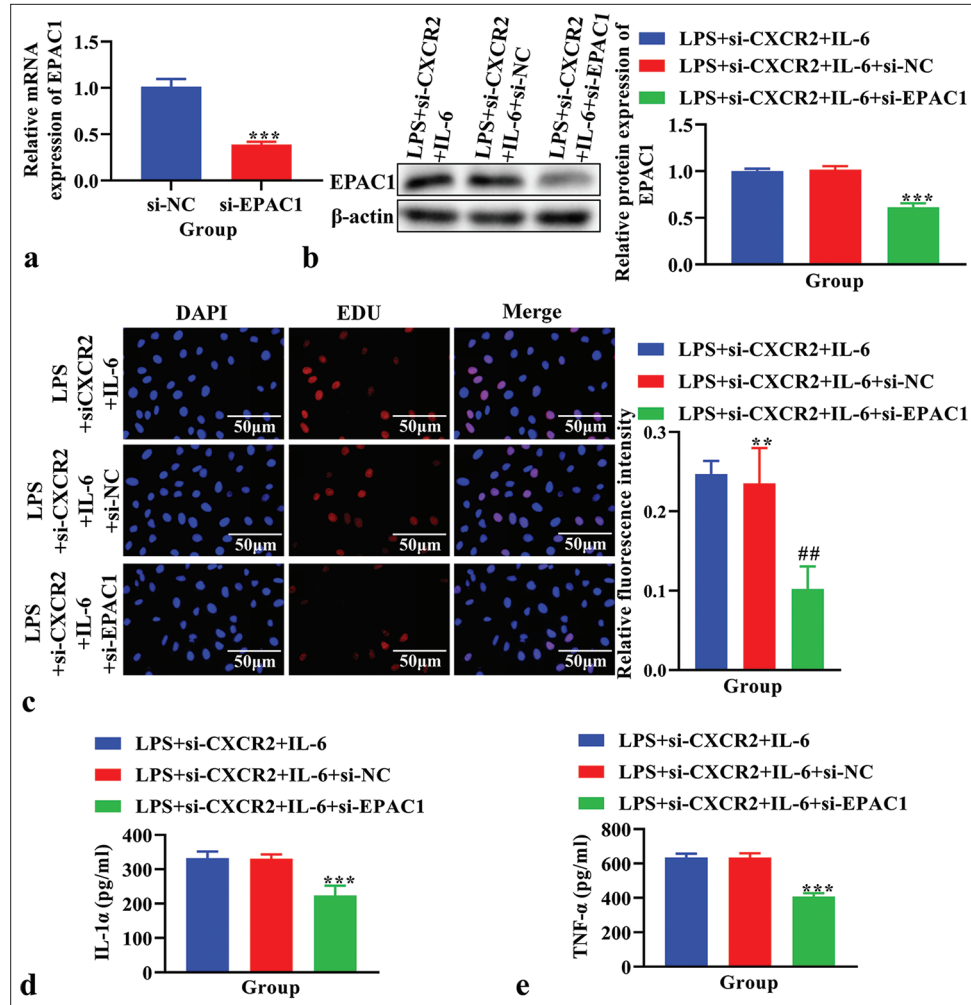


**Figure 6:** The effects of knockdown exchange protein 1 directly activated by cAMP (EPAC1) on cell proliferation, the level of interleukin (IL)-1 $\alpha$  and tumor necrosis factor- $\alpha$  (TNF- $\alpha$ ) in lipopolysaccharide (LPS)-induced primary microglia cells treated with si-C-X-C motif chemokine receptor 2 (CXCR2) and IL-6. (a) The expression of EPAC1 using real time polymerase chain reaction. \*\*\* $P < 0.001$  versus si-NC. (b) The expression of EPAC1 using western blot. (c) Cell proliferation using EdU assay. (d) The level of IL-1 $\alpha$  using enzyme linked immunosorbent assay (ELISA). (e) The level of TNF- $\alpha$  using ELISA. \*\* $P < 0.01$  \*\*\* $P < 0.001$  versus LPS+si-CXCR2+IL-6+si-NC. ## $P < 0.01$  versus LPS+si-CXCR2+IL-6+si-NC.

with the findings *in vivo*. Moreover, after adding IL-6, an activator of the JAK-STAT signaling pathway,<sup>[30]</sup> the downregulation of the JAK-STAT signaling pathway induced by si-CXCR2 was reversed, and the changes in IL-1 $\alpha$  and TNF- $\alpha$  levels were also reversed. However, si-EPAC1 reversed the above changes induced by IL-6, indicating that the downregulation of EPAC1 may promote the recovery of CPSP. Further, *in vivo* experiments are needed to verify that inhibition of CXCR2 may alleviate CPSP by reducing primary microglia proliferation, immune response, and regulating the JAK-STAT signaling pathway.

In addition, si-CXCR2 increases STAT3 while decreasing p-STAT3 may adjust the activity of STAT3 and its phosphorylation state in response to the negative feedback

mechanism of anti-inflammatory signaling to avoid excessive or inappropriate inflammatory response and, thus, maintain or restore normal physiological function of cells. These results suggest that si-CXCR2 may play an anti-inflammatory role by increasing the expression of STAT3 in the non-phosphorylated state and inhibiting the phosphorylation of STAT3. In contrast, some studies have shown that siCXCR2 eliminated the inhibition of STAT3 phosphorylation and inflammation by Jiawei Xiaochengqi decoction,<sup>[31]</sup> indicating that CXCR2 may have variable regulation modes. Further, quantitative statistics on the specific behavior of animal models after administration of CXCR2 inhibitors are needed to complement the features of CXCR2 in the CPSP model.

Recent studies have shown that CXCR2 regulates multiple signaling pathways, including Ras/ERK, PI3K/Akt, JAK2/STAT3, PLC/PKC, and mitogen-activated protein kinase (MAPK)/p38, each leading to distinct biological effects.<sup>[32]</sup> Among these, inhibiting the rat sarcoma viral oncogene homolog (RAS)/extracellular signal-regulated kinase (ERK) pathway triggers NFκB-dependent upregulation of CXCR2 ligands, which, in turn, suppresses T-cells.<sup>[33]</sup> The activation of CXCL1 stimulates CXCR2 in microglia to regulate the MAPK/p38 pathway involved in neuropathic pain.<sup>[34]</sup> In addition, CXCR2 activation promotes the expression of COX-2 through p-ERK, which regulates the peripheral nerve injury nociceptors.<sup>[35]</sup> In our study, we showed that CXCR2 aggravated CPSP by activating microglia through the JAK1/STAT3 signaling pathway, further confirming the key role of CXCR2 in neuropathic pain. Our findings supplement existing knowledge on related pathways and mechanisms, providing a new theoretical basis for whether CPSP is associated with neuropathic pain. However, we need to further explore the specific role and mechanism of the CXCL1/CXCR2 axis in CPSP<sup>[36]</sup> and investigate the etiology and treatment of CPSP.

## SUMMARY

This study showed that the downregulation of CXCR2 expression can decrease the levels of EPAC1 to suppress cell proliferation and immune response, thereby alleviating CPSP by inhibiting the JAK1/STAT3 signaling pathway. In the future, we will further validate the efficacy and safety of CXCR2 in alleviating CPSP using other experimental methods.

Our findings provide new targets for alleviating CPSP, specifically CXCR2, offering insights for developing new synergistic treatments based on their mechanisms of action. In addition, significant differences observed in the relevant indicators highlighted in the research findings could aid in diagnosing CPSP.

## AVAILABILITY OF DATA AND MATERIALS

The datasets used and/or analyzed during the current study are available from the corresponding author on reasonable request.

## ABBREVIATIONS

CPSP - Chronic post-surgical pain  
 CXCR2-C-X-C - Motif chemokine receptor 2  
 NC - Negative Control  
 IL - Interleukin  
 JAK - Janus Kinase  
 STAT - Signal Transducers and Activators of Transcription  
 EPAC1 - Exchange Protein 1 directly Activated by cAMP  
 LPS - Lipopolysaccharide  
 GEFs - Guanine nucleotide exchange protein conversion factor

SD - Sprague-Dawley  
 SMIR - Skin/muscle incision and retraction  
 CPCSEA - Committee for the Purpose of Control and Supervision of Experiments on Animals  
 PBS - Phosphate buffered saline  
 BSA - Bovine serum albumin  
 DAPI-4',6 - Diamidino-2-phenylindole  
 DMEM - Dulbecco's Modified Eagle Medium  
 TNF-α - Tumor necrosis factor-α  
 ELISA - Enzyme-linked immunosorbent assay  
 EdU - Ethynyl-2'-deoxyuridine  
 GO - Gene ontology  
 KEGG - Kyoto encyclopedia of genes and genomes database  
 PPI - Protein-protein interaction  
 RAPGEF3 - Rap Guanine Nucleotide Exchange Factor 3  
 PCR - Polymerase chain reaction  
 RIPA - Radio immunoprecipitation assay  
 PVDF - Polyvinylidene difluoride  
 SPSS - Statistical Package for the Social Sciences  
 LSD - Least Significant Difference tests  
 MAPK - Mitogen-activated protein kinase  
 RAS - Rat sarcoma viral oncogene homolog  
 ERK - Extracellular signal-regulated kinase

## AUTHOR CONTRIBUTIONS

JZ, CJ, ZC, JC, CZ, ML, YY, and YG: Jointly conducted the study concept and design, acquisition of data, or analysis and interpretation of data. JZ and CJ: Wrote the manuscript, visualised the data; YG and YY: Reviewed and revised the manuscript. JZ and YG: Applied for the funds. All authors contributed to editorial changes in the manuscript. All authors read and approved the final manuscript. All authors have participated sufficiently in the work and agreed to be accountable for all aspects of the work.

## ETHICS APPROVAL

The ethical standard of experiments was in accordance with the guidelines provided by the CPCSEA, and all the procedures were approved by the Animal Ethics Committee of the Laboratory Animal Center of Nantong University (IACUC20230215-1004).

## FUNDING

This work was supported by Jiangsu Provincial Research Hospital [YJXY2022044-YSB31] and the Postgraduate Research & Practice Innovation Program of Jiangsu Province [grant number KYCX23\_3433].

## CONFLICT OF INTEREST

The authors declare no conflict of interest.

## EDITORIAL/PEER REVIEW

To ensure the integrity and highest quality of CytoJournal publications, the review process of this manuscript was conducted under a **double-blind model** (authors are blinded for reviewers and vice versa) through an automatic online system.

## REFERENCES

- De Ridder D, Adhia D, Vanneste S. The anatomy of pain and suffering in the brain and its clinical implications. *Neurosci Biobehav Rev* 2021;130:125-46.
- McCarberg B, Peppin J. Pain pathways and nervous system plasticity: Learning and memory in pain. *Pain Med* 2019;20:2421-37.
- Terkawi AS, Ottestad E, Altirkawi OK, Salmasi V. Transitional pain medicine; new era, new opportunities, and new journey. *Anesthesiol Clin* 2023;41:383-94.
- Esses G, Deiner S, Ko F, Khelemsky Y. Chronic post-surgical pain in the frail older adult. *Drugs Aging* 2020;37:321-9.
- Gan TJ, Habib AS, Miller TE, White W, Apfelbaum JL. Incidence, patient satisfaction, and perceptions of post-surgical pain: Results from a US national survey. *Curr Med Res Opin* 2014;30:149-60.
- Qian J, Lin X, Zhou Z. Skin/muscle incision and retraction regulates the persistent postoperative pain in rats by the Epac1/PKC- $\beta$ II pathway. *BMC Anesthesiol* 2022;22:230.
- Kehlet H, Jensen TS, Woolf CJ. Persistent postsurgical pain: Risk factors and prevention. *Lancet* 2006;367:1618-25.
- Li T, Liu T, Chen X, Li L, Feng M, Zhang Y, *et al.* Microglia induce the transformation of A1/A2 reactive astrocytes via the CXCR7/PI3K/Akt pathway in chronic post-surgical pain. *J Neuroinflammation* 2020;17:211.
- Ruff MR, Inan S, Shi XQ, Meissler JJ, Adler MW, Eisenstein TK, *et al.* Potentiation of morphine antinociception and inhibition of diabetic neuropathic pain by the multi-chemokine receptor antagonist peptide RAP-103. *Life Sci* 2022;306:120788.
- Li J, Deng G, Wang H, Yang M, Yang R, Li X, *et al.* Interleukin- $\beta$  pre-treated bone marrow stromal cells alleviate neuropathic pain through CCL7-mediated inhibition of microglial activation in the spinal cord. *Sci Rep* 2017;7:42260.
- Acosta JC, O'Loughlin A, Banito A, Guijarro MV, Augert A, Raguz S, *et al.* Chemokine signaling via the CXCR2 receptor reinforces senescence. *Cell* 2008;133:1006-18.
- Zhang ZJ, Jiang BC, Gao YJ. Chemokines in neuron-glia cell interaction and pathogenesis of neuropathic pain. *Cell Mol Life Sci* 2017;74:3275-91.
- Piotrowska A, Rojewska E, Pawlik K, Kreiner G, Ciechanowska A, Makuch W, *et al.* Pharmacological blockade of spinal CXCL3/CXCR2 signaling by NVP CXCR2 20, a selective CXCR2 antagonist, reduces neuropathic pain following peripheral nerve injury. *Front Immunol* 2019;10:2198.
- Zhou W, Zhou Y, Wang M, Qian C, Wang C, Tang J, *et al.* Pharmacological inhibition of CXCR2 alleviates neuropathic pain by inactivating microglia in a rat L5 spinal nerve ligation model. *Am J Transl Res* 2020;12:3803-12.
- Simon LS, Taylor PC, Choy EH, Sebba A, Quebe A, Knopp KL, *et al.* The Jak/STAT pathway: A focus on pain in rheumatoid arthritis. *Semin Arthritis Rheum* 2021;51:278-84.
- Wang S, Li A, Guo S. Ligustrazine attenuates neuropathic pain by inhibition of JAK/STAT3 pathway in a rat model of chronic constriction injury. *Pharmazie* 2016;71:408-12.
- Pohóczyk K, Kun J, Szentes N, Aczél T, Urbán P, Gyenesei A, *et al.* Discovery of novel targets in a complex regional pain syndrome mouse model by transcriptomics: TNF and JAK-STAT pathways. *Pharmacol Res* 2022;182:106347.
- Cao S, Bian Z, Zhu X, Shen SR. Effect of Epac1 on pERK and VEGF activation in postoperative persistent pain in rats. *J Mol Neurosci* 2016;59:554-64.
- Hua Q, Shen S, Qin Y, Cao S. CAV-1 Overexpression Exacerbates the Manifestation in EPAC-1-Induced Chronic Postsurgical Pain in Rats. *Pain Res Manag.* 2022 Jul 31;2022:8566840.
- She Q, Chen J, Zhong C, Huang S, Lu C, Qin Y. Exchange proteins directly activated by cyclic adenosine monophosphate inhibitor reverses mechanical allodynia via the modification of astrocytes activity in the spinal cord. *Ann Transl Med.* 2021 Nov;9(22):1656.
- Hucho TB, Dina OA, Levine JD. Epac mediates a cAMP-to-PKC signaling in inflammatory pain: an isolectin B4(+) neuron-specific mechanism. *J Neurosci* 2005;25:6119-26.
- Gu Y, Li G, Chen Y, Huang LM. Epac-protein kinase C alpha signaling in purinergic P2X3R-mediated hyperalgesia after inflammation. *Pain* 2016;157:1541-50.
- Hylden JL, Wilcox GL. Intrathecal morphine in mice: A new technique. *Eur J Pharmacol* 1980;67:313-6.
- Pak DJ, Yong RJ, Kaye AD, Urman RD. Chronification of pain: Mechanisms, current understanding, and clinical implications. *Curr Pain Headache Rep* 2018;22:9.
- Chen H, She Q, Liu Y, Chen J, Qin Y, Lu C. The peripheral Epac1/p-Cav-1 pathway underlies the disruption of the vascular endothelial barrier following skin/muscle incision and retraction-induced chronic postsurgical pain. *Ann Transl Med* 2022;10:1377.
- Sun Y, Yang M, Tang H, Ma Z, Liang Y, Li Z. The overproduction of TNF- $\alpha$  via Toll-like receptor 4 in spinal dorsal horn contributes to the chronic postsurgical pain in rat. *J Anesth* 2015;29:734-40.
- Wei S, Han CZ, Wang J, Li K, Ru QM, Wang Y, *et al.* Repeated endomorphin analogue MEL-0614 reduces tolerance and improves chronic postoperative pain without modulating the P2X7R signaling pathway. *ACS Chem Neurosci* 2021;12:3124-39.
- Aihaiti Y, Cai YS, Tuerhong X, Yang YN, Ma Y, Zheng HS, *et al.* Therapeutic effects of naringin in rheumatoid arthritis: Network pharmacology and experimental validation. *Front Pharmacol* 2021;12:672054.
- Zhang Y, Chen Q, Nai Y, Cao C. Suppression of miR-155 attenuates neuropathic pain by inducing an M1 to M2 switch in microglia. *Folia Neuropathol* 2020;58:70-82.
- Heinrich PC, Behrmann I, Haan S, Herrmanns HM, Müller-Newen G, Schaper F. Principles of interleukin (IL)-6-type cytokine signaling and its regulation. *Biochem J* 2003;374(Pt 1):1-20.
- Liu W, Wu F, Bi X, Hou L, Wang C, Li Y, *et al.* Herbal formula Jiawei Xiaochengqi decoction prevents postoperative abdominal adhesion in a rat model through inhibition of

- CXCL2-CXCR2 pathway. *Phytomedicine* 2023;111:154662.
32. Xie Y, Kuang W, Wang D, Yuan K, Yang P. Expanding role of CXCR2 and therapeutic potential of CXCR2 antagonists in inflammatory diseases and cancers. *Eur J Med Chem* 2023;250:115175.
  33. Tang KH, Li S, Khodadadi-Jamayran A, Jen J, Han H, Guidry K, *et al.* Combined inhibition of SHP2 and CXCR1/2 promotes antitumor T-cell response in NSCLC. *Cancer Discov* 2022;12:47-61.
  34. Moraes TR, Elisei LS, Malta IH, Galdino G. Participation of CXCL1 in the glial cells during neuropathic pain. *Eur J Pharmacol* 2020;875:173039.
  35. Jiang S, Liang J, Li W, Wang L, Song M, Xu S, *et al.* The role of CXCL1/CXCR2 axis in neurological diseases. *Int Immunopharmacol* 2023;120:110330.
  36. Carreira EU, Carregaro V, Teixeira MM, Moriconi A, Aramini A, Verri WA Jr., *et al.* Neutrophils recruited by CXCR1/2 signalling mediate post-incisional pain. *Eur J Pain* 2013;17:654-63.

**How to cite this article:** Zhao J, Jian C, Chen Z, Cai J, Zhou C, Li M, *et al.* Inhibition of CXCR2 as a therapeutic target for chronic post-surgical pain: Insights from animal and cell models. *CytoJournal*. 2024;21:28. doi: 10.25259/Cytojournal\_46\_2024.

HTML of this article is available FREE at:  
[https://dx.doi.org/10.25259/Cytojournal\\_46\\_2024](https://dx.doi.org/10.25259/Cytojournal_46_2024)

The FIRST **Open Access** cytopathology journal

Publish in *CytoJournal* and **RETAIN** your *copyright* for your intellectual property  
**Become Cytopathology Foundation (CF) Member at nominal annual membership cost**

For details visit <https://cytojournal.com/cf-member>

PubMed indexed  
**FREE** world wide **open access**  
**Online processing** with rapid turnaround time.  
**Real time** dissemination of time-sensitive technology.  
Publishes as many **colored high-resolution images**  
Read it, cite it, bookmark it, use RSS feed, & many----



**CYTOJOURNAL**

[www.cytojournal.com](http://www.cytojournal.com)

Peer-reviewed academic cytopathology journal





# NextGen CelBloking™ Kits

**Frustrated with your cell blocks?  
We have a better solution!**

**Nano**

## Nano NextGen CelBloking™

Cell block kit to process single scattered cell specimens and tissue fragments of **any** cellularity.



**PATENT PENDING**



**Pack #1**



**Pack #2**

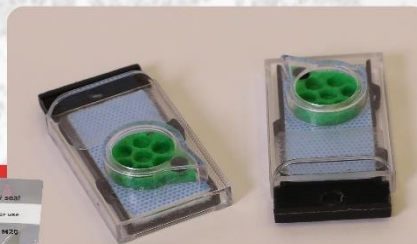
**Micro**

## Micro NextGen CelBloking™

For cellular specimens (more than 1 ml concentrated specimen with Tissuecrit more than 50%)



**PATENT PENDING**



**Pack #1**



**Pack #2**